Determining 1:1 Charge Stoichiometry and Rheological Characterization for pH Induced Chitosan-*Albizia procera* Complex Coacervate Xerogels

Dr. Partha Sarathi Roy *

Posted Date: 1 August 2024

doi: 10.20944/preprints202407.2533.v1

Keywords: polyelectrolyte complex (PEC) coacervate xerogels; strain sweep; frequency sweep; storage modulus

Article

Determining 1:1 Charge Stoichiometry and Rheological Characterization for pH Induced Chitosan-*Albizia procera* Complex Coacervate Xerogels

Partha Sarathi Roy [1,2,†]

[1] University of Missouri-Kansas City, Health Sciences Building (HSB), Division of Pharmaceutical Sciences, 2464 Charlotte St., Kansas City, MO, 64108-2718, United States; parthasarathi.r@snuniv.ac.in
[2] University of the Pacific: Thomas J. Long School of Pharmacy and Health Sciences, Department of Pharmaceutics/Medicinal Chemistry, 751 Brookside Rd, Stockton, CA, 95211, United States
[†] Present Address: Sister Nivedita University, School of Pharmacy, Newtown, Kolkata, West Bengal, 700156, India.

Abstract: In order to explore new options for colon targeting, this study designs new polyelectrolyte complex (PEC) coacervate xerogels of chitosan (Ch) with *Albizia procera* (AP). It was determined by potentiometric titration tests that a 1:5 Ch/AP weight ratio was necessary for 1:1 charge stoichiometry. Rheological characterizations experiments were carried out for the pH independent coacervates and 1:5 coacervate was found to be having the highest G/ value in the strain sweep experiment. In the frequency sweep experiments the coacervate (1:5) with the highest storage modulus (G/) values was produced at pH 4.5.

Keywords: polyelectrolyte complex (PEC) coacervate xerogels; strain sweep; frequency sweep; storage modulus

1. Introduction

The assembly of oppositely charged polymers or particles is essential to many established and developing technologies. Charge complexation in solution may be involved in such an interaction. The term "coacervation," which was first used by Bungenberg de Jong and Kruyt [1] in their groundbreaking work, comes from the Latin word "acervus," which meaning aggregation (a heap), plus the prefix "co" (together), which denotes the previous union of the colloidal particles [2]. Coacervation, according to IUPAC, is the division of a colloidal system into two liquid phases: the equilibrium solution and the coacervate, which is the phase with the highest concentration of the colloid component [3]. There are two categories for this phenomenon: "simple" and "complex" coacervation. In short, simple coacervation is the process of adding a very hydrophilic material to a colloid solution, resulting in the formation of two phases: one phase rich in colloidal droplets and the other poor in such droplets. It is typically applied to systems with a single colloidal solute. The main factor influencing this process is the level of hydration generated, which is a tough to regulate variable. The division of a macromolecular solution made up of two oppositely charged macroions into two immiscible liquid phases, on the other hand, is known as complex coacervation. The term "complex coacervation" was introduced by Bungenberg de Jong and Kruyt [1] to differentiate it from the simple coacervation of a single polymer. It has been observed that complex coacervation is predominantly reliant on pH [4,5]. Complex coacervation is thought to occur by the electrostatic interaction of oppositely charged polyelectrolytes [6–8] and oppositely charged colloids, such as micelles, proteins, or dendrimers and independent of temperature [9]. Charge neutralization, such as by changing the charge of one or both partner macroions or the combining ratio (microstoichiometry) inside the complex, is typically the first step toward coacervation for both systems. Determining the

 doi:10.20944/preprints202407.2533.v1

degree to which the simultaneous aggregation is a result of neutralization or a genuine prerequisite for coacervation can be challenging. In either case, it is evident that the coacervate yield is maximum for both types of macroions in the region of (bulk) 1:1 charge stoichiometry ("[+]/ [−])" [10–12]. Because the most salt bonds occur at this pH, the ideal circumstances for complex coacervation are reached when the pH is changed to a point at which equivalents of oppositely charged molecules of the two polyelectrolytes/colloids are present [13,14]. A number of scientists proposed several years ago that the coacervate phase may act either like an elastic gel or like a concentrated solution (viscous behavior), which presented the intriguing subject of the coacervate phase's rheological features.9. From a rheological perspective, the storage modulus (G') and loss modulus (G'') in the viscous fluid (sol state) are $G'' > G.$, and in the elastic gel state, $G'(\omega) > G''(\omega)$ [15–18]. It is reported that an elastic solid state (gel) has an infinite network while a viscous fluid state (sol) contains only finite branched clusters. The network can originate from noncovalent interactions like electrostatic/ionic interactions, helical domains, micro-crystalline bundles, hydrogen bonding, coordination, crystallization, hydrophobic effect, and so on (physical or reversible gels) or from covalent structure (chemical or irreversible gels). [19–21] Given that the electrostatic contacts within PEC gels are significantly stronger than those inside most secondary binding interactions, polyelectrolyte complex coacervates (PEC) are known to exhibit distinct physical and chemical features. [22]

As a heterogeneous binary polysaccharide consisting of β- (1,4) 2-amino-2-deoxy-β-D-glucopyranose units with partial β- (1,4)-linked 2-acetamido-2-deoxy-β-D-glucopyranose, chitosan (Ch) can form polyelectrolyte complexes through electrostatic interaction with anionic groups of anionic polysaccharides (usually carboxylic acid groups) [23]. These polyelectrolyte complexes have been widely administered orally [24]. Because chitosan is less immunogenic than synthetic polymers and is nontoxic, mucoadhesive, biocompatible, and biodegradable, it has great promise for usage in the food industry and in both conventional and innovative gastrointestinal drug delivery systems [25]. Creating these cross-linked polyelectrolyte complexes by the interaction of chitosan with additional polysaccharides such chondroitin, carrageenan, xanthan gum, sodium alginate, polyvinyl alcohol, pectin, and gum kondagogu has garnered more attention in recent years. The pharmaceutical, food, and biotechnology sectors are among those with a large number of PEC uses. The particular use of these compounds depends on their rheological and structural characteristics. One of the primary uses of complicated coacervation, for instance, is the creation of regulated release carriers, where the predominance of elastic behavior over viscous activity is viewed as a benefit. A polyelectrolyte complex of chitosan and other polymers has the benefit of not requiring chemical cross-linking agents or organic solvents, which lowers toxicity and unfavorable side effects [26].

The extremely significant multipurpose tree legumes that make up the subfamily Mimoseae of the family Leguminosae include the genus *Albizia*. There are about 150 species in it, with deciduous woody trees and shrubs making up the majority of the species [27]. In Central America, *Albizia* trees are highly prized for their use as lumber trees, water-soluble gum suppliers, stabilizers of soil erosion, understory shade trees for crop plantations, and soil improvers [28]. Ayurvedic medicine also places great value on certain species of *Albizia* trees, including *A. julibrissin*, *A. lebbeck*, *A. procera*, and *A. amara* [29]. A naturally occurring polysaccharide that is a member of the Leguminosae family is gum *Albizia stipulata* (AS) [30]. There are about 150 species in the genus *Albizia*, the majority of which are woody, deciduous trees and shrubs. *Albizia lebbeck* gums, which are produced by *Albizia* trees, have been claimed to be natural emulsifiers that can replace arabic gum in the food and pharmaceutical industries [31]. *Albizia zygia* gum has been used as a binding agent [32] in tablet formulations and in the formulation of pharmaceutical solutions [33]. *Albizia procera* gum has been described as an excipient for oral controlled-release matrix tablets [34]. Due to the diverse range of *Albizia* species found worldwide, *Albizia* gums have the potential to be more affordable and renewable than other industrial gums [35]. A lot of research has been done on *Albizia* gums as a potential gum Arabic replacement [36,37]. *Albizia* gums are composed of a primary chain of β(1-3) D-galactose units, some β (1-6) linked D-galactose units, and α(1-3) L-arabinose units, according to partial structural studies [36,38].

 doi:10.20944/preprints202407.2533.v1

The treatment of diseases of the large intestine, including Crohn's disease, ulcerative colitis, irritable bowel syndrome, colon cancer, and amebiasis, is one of the major therapeutic uses of colon targeted delivery systems. Chitosan has recently demonstrated potential as a carrier in colon targeting; data point to the possibility that one of chitosan's key characteristics for effective colon targeting application is conjugation with a range of substrates via its amine. But according to Okamoto et al. [39], chitosan's strong biodegradability in acidic environment meant that it quickly disintegrated in the stomach cavity, making it incapable of preventing degradation. As a result, it was unable to safeguard the drug load during transit through the stomach and small intestine. When taken as a whole, our analyses offer a comprehensive understanding of how the degree of interaction between Ch and *Albizia procera* (AP), as well as rheological characterisation, may impact future applications, especially when it comes to the creation of possible colon-specific drug delivery vehicles. As far as we are aware, no other research has provided such a thorough description of the Ch−AP PEC coacervates.

2. Materials and Methods

2.1. Materials

It has been observed that raising the molecular weight of chitosan enhances PEC formation because of a chain entanglement effect, which relates to the impacts of chitosan molecular weight on the interactions with polyanions [40]. After the initial electrostatic contact has taken place, high molecular weight chitosan with longer chains and more charges can more readily entangle and trap free AP, leading to the development of PEC. Thus, high molecular weight chitosan powder (MW = 161,000 g/mol, degree of deacetylation >75%, Sigma-Aldrich, Milwaukee, WI, USA) was chosen for this investigation. The following materials were provided by their respective companies: sodium hydroxide anhydrous pellets (NaOH) (Amresco Co., Solon, OH, USA), ether (C_2H_5–O–C_2H_5), and absolute ethanol (C_2H_6O) (Merck, Darmstadt, Germany). These materials were utilized without additional purification. The analytical reagent-grade hydrochloric acid (HCl, 37% w/w) was acquired from Carlo Erba Co., Ltd. in Milan, Italy.

2.2. AP and Chitosan Purification : Making Stock Solutions

With a few minor adjustments, the gum was purified using the technique that a group had previously published [35]. In short, 80% ethanol was boiled with the raw gum powder to dissolve low molecular weight carbohydrates and enzymes, as well as coloring agents. It was added to deionized water and swirled gently with a magnetic stirrer for the entire night. After that, the gum solution was let to stand at room temperature for 12 hours in order to extract any remaining material. After that, the gum solution was filtered through three folds of muslin fabric, and three times as much propanol was added to the solution to precipitate the gum. Following collection and air drying, the precipitate was run through sieve no. 85, which has a nominal mesh aperture size of 180 m. In preparation for additional analysis, the refined material was kept in a desiccator.

As previously reported [41], Chitosan (Ch) was purified by dissolving in a 0.2 M acetic acid solution (5 g L^{-1}) and then filtering through membranes (3, 1.2, and 0.8 μm) and sintered glass filters (pore diameters up to 16 μm). After that, it was precipitated by gradually adding 1 M ammonium hydroxide until the pH reached around 9 (as determined by a WTW pH330, Germany pH meter at 25 °C). It was then thoroughly cleaned with water until the conductivity did not change, and it was then further cleaned with ethanol at concentrations of 70, 80, 90, and 100% (v/v). Finally, the refined polymer was dried at room temperature in a vacuum.

By dispersing the former in Milli-Q-grade water (18.0 mΩ) with 0.1 N HCl and the latter in Milli-Q-grade water, stock solutions of Ch (2 wt%) and AP (10 wt%) were created. For 12 hours, the solutions were gently mixed, and then they were kept overnight at 4 °C to guarantee that the biopolymers were completely hydrated.

2.3. pH's Impact on Coacervate Yield during Potentiometric Titration and Coacervate Preparation.

 doi:10.20944/preprints202407.2533.v1

In a Metrohm AG (Herisau, Switzerland) water-jacketed titration tank thermostated at 25.0 (±0.1) °C with a microburet in the presence of an inert atmosphere (N2), the solutions were titrated using standardized 0.5 mL of 0.1 N NaOH. Titrating with a conventional 0.01 N HCl solution allowed for the accurate determination of the base concentration. Two doses were given with a 60-second interval in between to make sure the reaction had achieved equilibrium. Potentiometric titrations were carried out using a 665 DOSIMATE (Metrohm AG) microburet, recording the results with a pHM 95 potentiometer (±0.1 mV) (Radiometer Analytical SAS, Lyon, France) at minimal volume increments of 0.001 mL. The titration curve's inflection point was used to estimate the potentiometric titration termination point. AP−Ch coacervate was made by mixing the two polysaccharide solutions in the required amounts, which were calculated using their equivalency point values. This allowed the functional groups to be charged neutrally. In order to ascertain the impact on the coacervate yield, the biopolymer solution that yielded the maximum coacervate yield under natural pH solution conditions was adjusted to pH 1–10 by adding either HCl (0.1 N) or NaOH (0.1 N) as needed. For twenty-four hours, the combined solutions were swirled at room temperature (25 ± 1 °C). In order to determine the complex weight, complex coacervates were separated by centrifugation (15000g, 10 min, Ultracentrifuge Sorvall RC 5C plus, Waltham, MA, USA). They were then cleaned with deionized water, dried under vacuum, and weighed.

2.4. Rheological Characterization

Using cone plate geometry on a peltier plate, rheological tests of the coacervates were conducted using an Anton Paar rheometer. Cone dimensions were 40 mm in diameter, $4^0\,00'\,22''$ in cone angle, and 121 μm in truncation. At 25 °C, the trials were conducted. We encased the sample chamber inside a box with a single hole for the sample cell axis and continuously supplied nitrogen gas flow into the box since it was challenging to enclose the entire rheometer in a glovebox in an inert atmosphere. There were two different kinds of studies carried out: a % strain sweep and a frequency sweep. To identify the linear viscoelastic zone, the amplitude strain sweeps (0.1−100%) were examined at an angular frequency (ω) of 10 rad s^{-1}. When the value of G' or G'' did not change for at least three consecutive experimental points as the strain percent increased, the region was deemed linear viscoelastic on the modulus−strain percent plots. The nonlinear viscoelastic region was thought to have begun at the linear viscoelastic region's final experimental point. It was determined that the modulus-strain percent curve's steepest downward inflection point began to characterize the nonviscoelastic zone the best. The frequency sweep studies were conducted within an expanded 0.1−100 rad s^{-1} angular frequency (ω) domain. The equipment software yielded the storage modulus (G') and the loss modulus (G'') in every scenario. The experimental data was plotted using Origin Scientific Graphing and Analysis Software version 8.5 (OriginLab Corp., Northampton, MA, USA) to create plots of G' − strain %, G'' −strain %, G' −ω, and G'' −ω.

3. Results and Discussion

3.1. Equivalence Point and Effect of pH on Coacervate Yield

A rapid way to determine the stoichiometric charge ratio of the polycation/polyanion interactions needed to generate an electrostatic complex is using potentiometric titration [42,43]. The inflection point from the titration curves of the biopolymer stock solutions was used to calculate the equivalency point of the biopolymer solutions (Figure 1a,b). NaOH generally dissociates entirely when titrated into the biopolymer solution, forming sodium cations and hydroxide anions that neutralize the $-COO^-$ and $-NH_3^+$ groups, respectively. Figure 1a,b makes it evident that the stock solutions containing 2 weight percent Ch and 10 weight percent AP had 0.4 mequivalents (mEq) of NaOH each.

 doi:10.20944/preprints202407.2533.v1

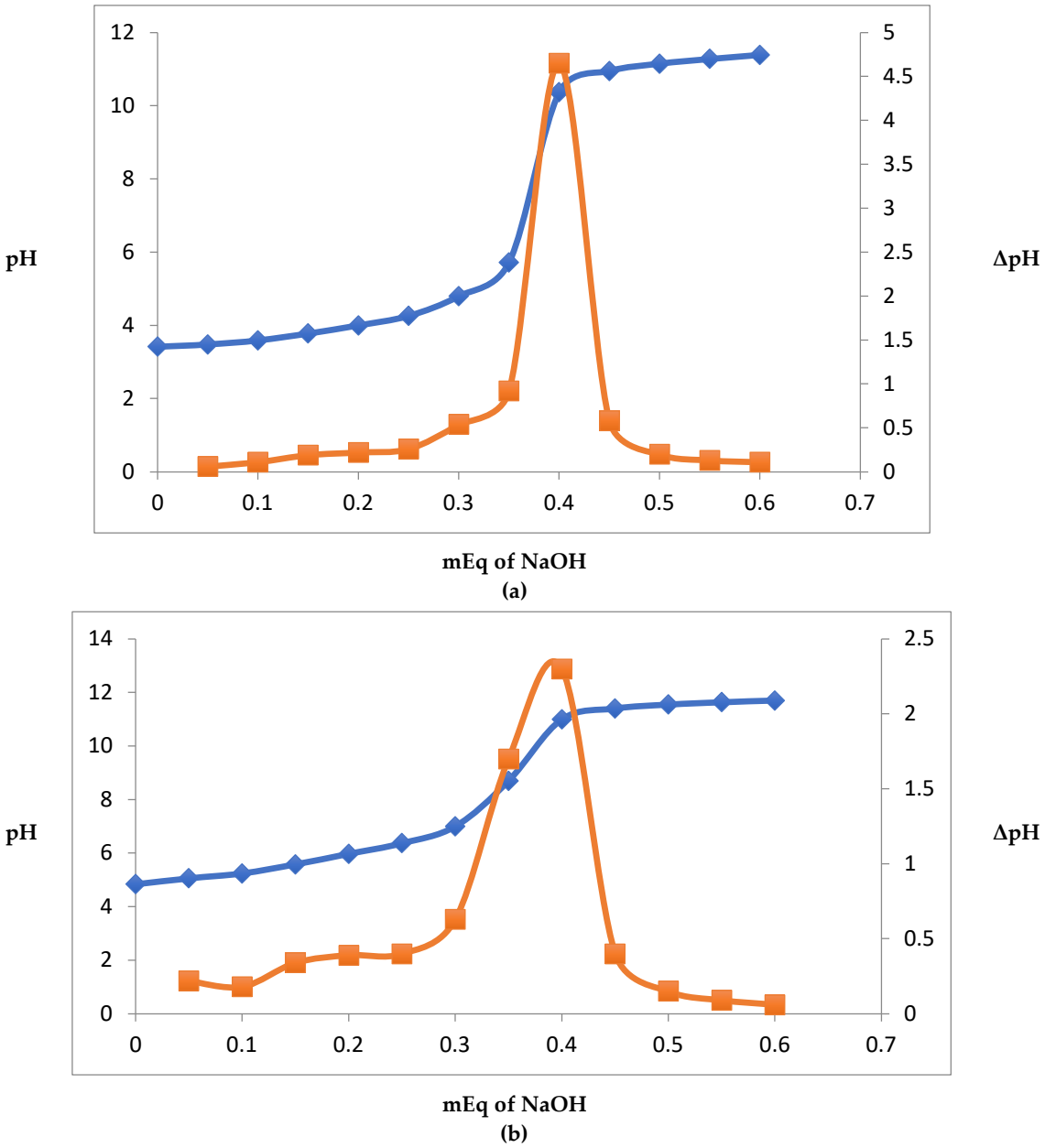

Figure 1. (a) Milliequivalent (mEq) of NaOH per 10 g of AP; (b) mEq of NaOH per 2 g of chitosan (note that both 10 wt % AP and 2 wt % chitosan stock solutions had 0.4 mEq NaOH).

The milliequivalent ratio of AP–Ch is displayed in Figure 2a as a function of the initial pH-independent ratios of the AP–Ch complexes (also see Table 1). Interestingly, each milliequivalent ratio is 2×10^{-1} times the starting ratio of the biopolymer. When the two polysaccharides are combined at a ratio that maximizes the attraction force between them and ensures that their opposing charges have the same magnitude, the maximum interaction takes place. Complex coacervation occurs when the ionized groups of both macromolecules are mutually neutralized, resulting in the formation of insoluble complexes. The highest coacervation, measured in terms of coacervate yield, happens at the equivalent mixing ratio/stoichiometric charge ratio of polysaccharides (1:1/"[+]/[−])"), or 5 g AP/g Ch. The predominance of free amine groups (occurring when the biopolymer initial ratios were <5) and a larger amount of ionized carboxyl moieties (occurring when the biopolymer initial ratios were >5) in the solution, as well as a more noticeable decrease in coacervate yield, cause the charge balance between the macromolecules to drift further away from its stoichiometric ratio as the biopolymer ratio moves further away from 5. Several systems, including pectin and β-lactoglobulin, lysozyme and sodium polystyrene sulfonate, PDADMAC, and BSA, were shown to exhibit coacervation with

 doi:10.20944/preprints202407.2533.v1

stoichiometry [10]. As seen in Figure 2b, the coacervate yield for a Ch−AP 1:5 system was impacted by pH. Since the biopolymer charge densities of the opposite sign appear to be stoichiometrically balanced at pH 4.5, the compensate yield attained was considerably greater (77%) than those at other pH values. This pH is quite similar to the "natural" biopolymer solution pH, which fell within a value of 4.3 ± 0.1. The coacervate yields (%) versus pH behavior (Figure 1d) shows that both the net charge of biopolymers and the stoichiometry of their electrostatic complexes are impacted as pH values deviate from 4.5. This results in a reduction in coacervate yield and, ultimately, the appearance of soluble complexes. As an illustration, Figure 1d displays the declining coacervate (%) yields in relation to descending pH as follows: pH 4.5 (77%) > pH 4.0 (70%) > pH 3.5 (69%) > pH 3 (65%). Several authors have reported on the dependence of coacervation on pH [44,45] They discovered that changes in pH led to a shift in the net charge of the biopolymers, which in turn caused conformational changes in their backbones and a reduction in the number of sites available for moiety interaction (weak interparticle interaction). An anionic polysaccharide is enriched in the insoluble complexes as the pH drops, per a study by Tolstoguzov [46]. We believe that two phenomena—i) protonation of the AP carboxylic groups and (ii) contraction of the macromolecular backbone—caused the coacervate yield to decrease at pH values below 4.5. These phenomena appear to peak at pH 2.5, at which point coacervation is completely inhibited. Conversely, the coacervate yields (%) decline at pH values above 4.5, exhibiting the following order: pH 4.5 (77%) > pH 5 (73%) > pH 5.5 (71%) > pH 6.0 (68%) > pH 6.5 (62%) > pH 7.0 (57%). This is primarily due to the chitosan molecules' decreased degree of ionization as they get closer to their pKa value (6.3–7) [47], and the maximum degree of AP molecules' ionization at pH 7 [48]. The observed variation in the elastic behavior of the networks with pH variation could be explained by changes in the electrostatic composition (see Rheological Characterization).

Table 1. Ratio of AP− Ch Milliequivalents (mEq) as a Function of AP−Ch Initial Ratio[a].

biopolymer ratio (GA: Ch)	mEq of NaOH (AP)	mEq of NaOH (Ch)
1-1:1	0.2	0.4
2-2:1	0.25	0.4
3-3:1	0.3	0.4
4-4:1	0.35	0.4
5-5:1	**0.4**	**0.4**
6-6:1	0.45	0.4
7-7:1	0.5	0.4

[a]The acquired 1:1 mEq ratio at a 5:1 AP− Ch ratio is represented by the bold values. Details can be found in Figure 2a.

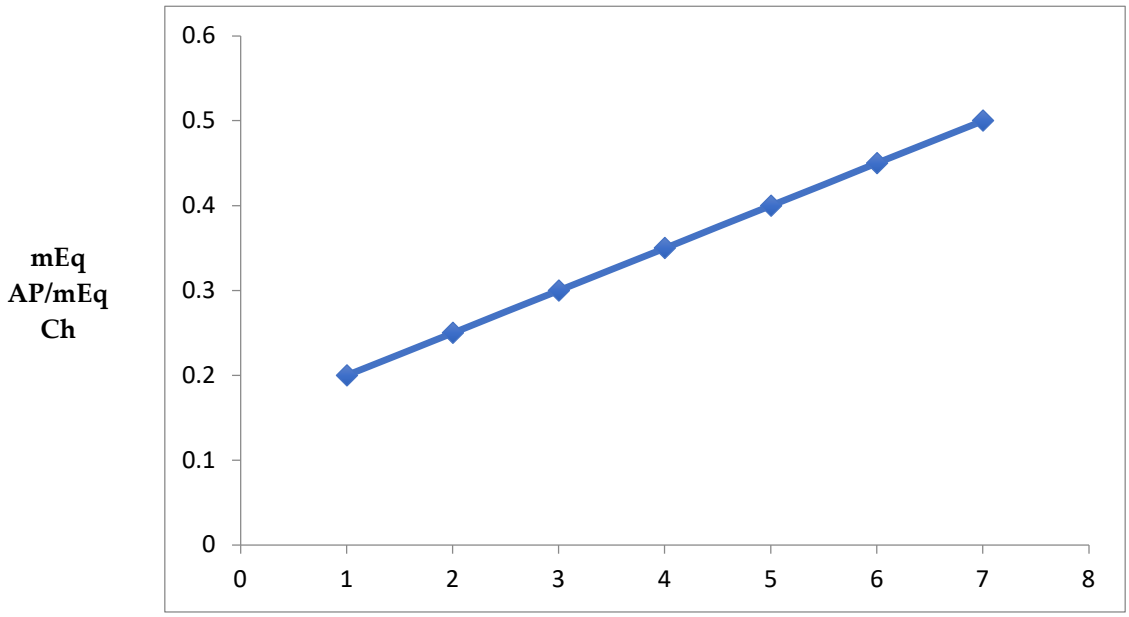

 doi:10.20944/preprints202407.2533.v1

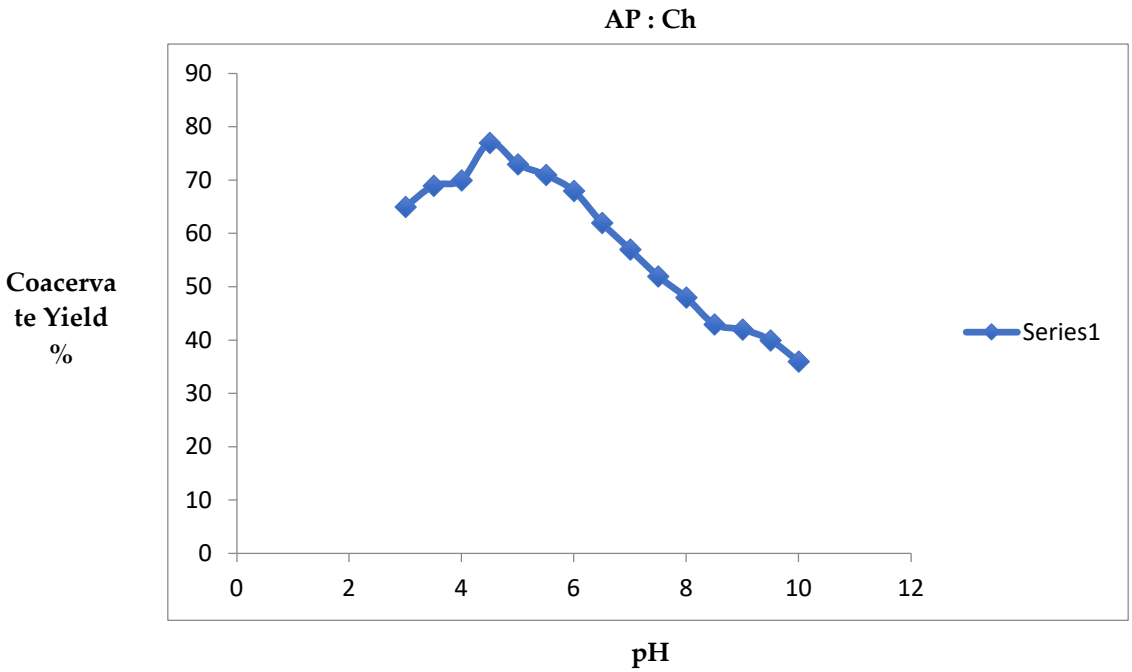

Figure 2. (a) AP − Ch mEq ratios as a function of initial AP–Ch ratio (note that the mEq ratio equals 1:1 at a biopolymers ratio of 5 (5:1 ratio of AP and Ch); (b) Ch – AP (1:5 system) coacervate yield as a function of induced pH (1–10) and after 24 h.

3.2. Rheological Characterization

In order to ascertain the linear viscoelastic range of the pH-independent Ch–AP PEC coacervates, strain sweeps were conducted for 1:4, 1:5, and 1:6 systems at an angular frequency (ω) of 10 rad s^{-1}. The linear viscoelastic area was found in all of the systems up to a maximum strain percent of 10, according to the G′ data (Figure 2a-c). A linear zone with a constant value of G/ at low strain % and a strong downward inflection in G/ at larger strains are characteristics of the PECs. The movement of the inflection point indicates the amount of stress that the PEC can bear before breaking, which may indicate the PEC body dissolution. Additionally, depending on the structure network inside the systems, bonds break and reformat at various rates when strains surpass that of the linear viscoelastic zone, resulting in a variation in G/ values. The critical strain (% γ) values for pH 1:5, 1:6, and 1:4 systems are 13.86, 8.0, and 7.52, respectively, determined by finding the junction of the two linear sections of the G/ vs. % strain plot. The linear viscoelastic region's storage modulus (G/) magnitudes exhibit a falling order of 1:5 (986 Pa) > 1:6 (780 Pa) > 1:4 (676 Pa). Given that G/ and critical strain have the same sequence, it can be deduced that the 1:5 system has the maximum mechanical strength, the 1:4 system the lowest, and the 1:6 system the intermediate strength. Its increased mechanical strength is clearly explained by the maximum degree of contact between the biopolymers in the 1:5 system. Figure 3 presents a comparison of the pH independent coacervates' loss modulus (G//) vs strain behavior. The curves exhibit comparable patterns and forms to the G//–strain percent curves. In the linear viscoelastic area, the loss modulus values were 1:5 (265 Pa) > 1:6 (154 Pa) > 1:4 (32 Pa), arranged in descending order. It was evident that the value of G/ was much bigger than G// at a given strain percent in the linear viscoelastic zone, suggesting a dominantly elastic nature for the PEC [15–18]. We fixed a constant strain of 1% to perform the frequency sweeps based on these findings.

 doi:10.20944/preprints202407.2533.v1

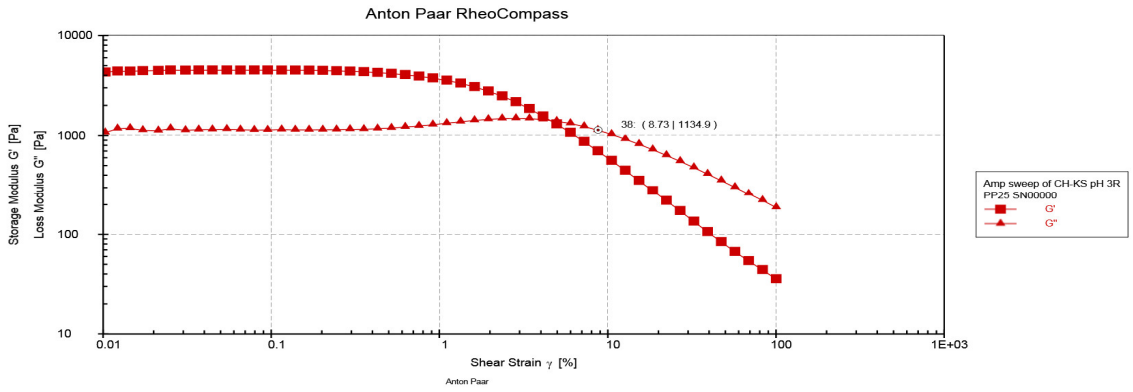

(**a**)

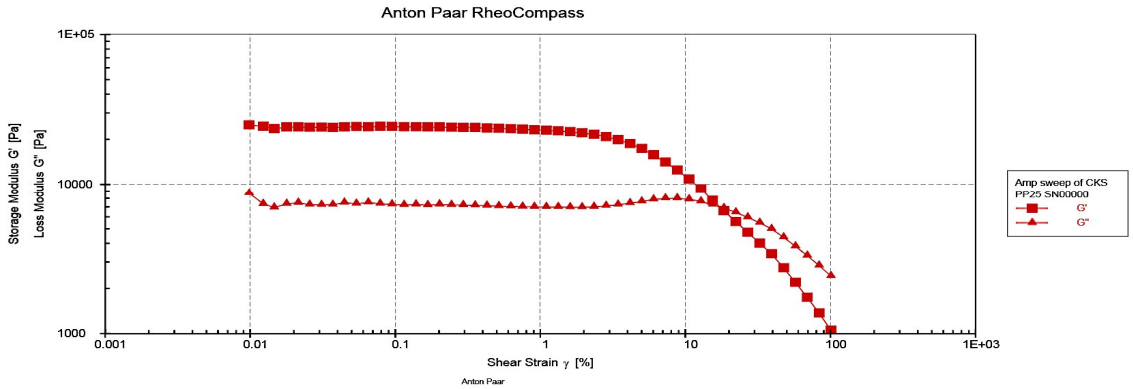

(**b**)

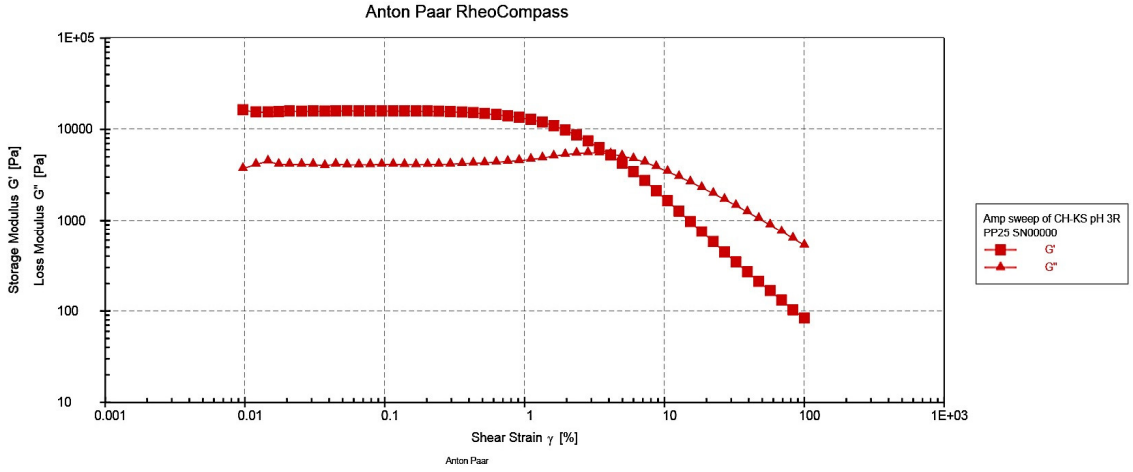

(**c**)

Figure 3. pH-independent Ch−AP Variation [1:4 (4.6 ± 0.0), 1:5 (4.2 ± 0.1), and 1:6 (3.6 ± 0.0)] were the original pH values. As a function of strain percentage, PEC exacerbates the following rheological properties: (a) storage modulus G/ and loss modulus G// for 1:6 system; (b) G/ and G// for 1:5 system; (c) G/ and G// for 1:4 system.

 doi:10.20944/preprints202407.2533.v1

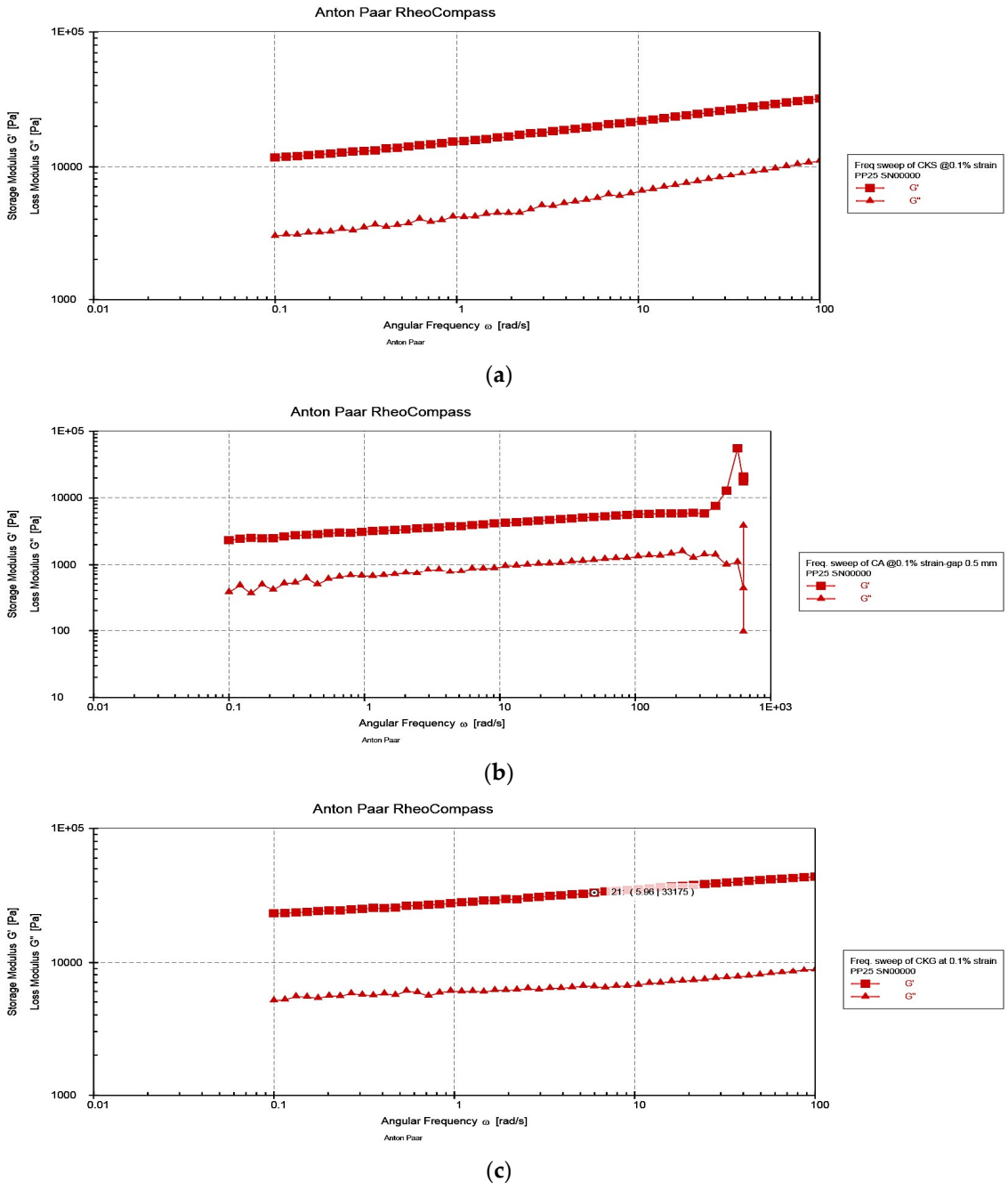

Figure 4. Frequency sweeps of the Ch-AP (1:5) PEC coacervates at 25 °C caused by pH (3.0, 6.0, and 4.5 (a-c)).

The frequency sweep curves of Ch−AP coacervates in the linear viscoelastic zone at various pH levels are displayed in Figure 3. The oscillatory parameters utilized to compare the viscoelastic qualities for all of the coacervate systems were the storage modulus (G/), which is a measure of elastic nature; the loss modulus (G″), which is a measure of viscous nature; and the loss tangent (tan δ = G″/G′). The fact that the value of G′ was significantly bigger than G″ and the loss tangent (tan δ = G″/G′) was less than 1 throughout the whole frequency range under study for pH 4.5 and 6 induced Ch−AP 1:5 systems is particularly intriguing. Thus, this pattern suggests that these systems are primarily elastic. The same analysis was then embraced by three more groups as the main reason for the dominating elasticity [49–51]. The G′ values of the pH 4.5 system grow more quickly than the pH 6.0 system with increasing frequency, even though at low frequencies the G′ values of both systems are the same (Figure 3). Nevertheless, we fail to detect any crossover zone between G′ and G// in any of these experiments, suggesting the lack of a gel−sol transition. The strongest connection between

 doi:10.20944/preprints202407.2533.v1

the two biopolymers may be the main cause of the pH 4.5 system's maximum elastic mechanical response (see Equivalency Point and Effect of pH on Coacervate Yield; Figure 2). These findings should be considered while developing formulations for colon targeting. Other coacervates, such as β-lactoglobulin–xanthan gum [52], bovine serum albumin (BSA)–poly(diallylmethylammonium chloride) (PDMDAAC) [53], pectin–β-lactoglobulin [54], and pectin–poly-L-lysine, have also been found to exhibit a primarily elastic gel characteristic [55].

4. Conclusions

The electrostatic complex coacervates of chitosan with *Albizia procera* that we prepared in our experiments are promising as potential materials for colon targeting. The chitosan- *Albizia procera* complex coacervation performed best at a weight ratio of 1:5 (1:1 charge stoichiometry), according to potentiometric titration. However, the maximum interaction between the two biopolymers happened in a pH 4.5-induced 1:5 system, which is extremely close to the pH of the "natural" biopolymer solution. The greatest findings of elastic mechanical strength were found for a 1:5 complex coacervate system, according to the pH-independent strain sweep curves. Furthermore, the frequency sweep curves demonstrate that the coacervate produced at pH 4.5 exhibits the strongest elastic mechanical response. Therefore, it would seem that there are hallmark interactions between the biopolymers and the rheological behavior of their PEC coacervates for maximum PEC coacervation process.

Author Contributions: Present Address: [§]P.S.R.: *Department of Pharmaceutical Chemistry, School of Pharmacy, Sister Nivedita University, Newtown, Kolkata, West Bengal, 700156, India*; Email: royps2005@yahoo.com; parthasarathi.r@snuniv.ac.in

Acknowledgments: P.S.R gratefully acknowledges the postdoctoral research assistantships provided by University of the Pacific (UoP)-Stockton, California, and University of Missouri-Kansas City (UMKC), U.S.A. Additional support from the University Grants Commission (UGC), Government of India, New Delhi, India, for funding doctoral work with a Junior Research Fellowship (JRF) in Engineering and Technology [Fellowship 10-01/2008 (SA-I)] and a postdoctoral fellowship through the RUSA 2.0 scheme (Ref. No. R-11/214/19) are also gratefully acknowledged.

Conflicts of Interest: The authors disclaim any financial conflicts of interest.

References

1. Bungenberg de Jong, H. G.; Kruyt, H. R. Coacervation (partial miscibility in colloid systems). *Proc. Koninkl. Med. Akad. Wetenschap* **1929**, *32*, 849–856.
2. Sanchez, C.; Mekhloufi, G.; Schmitt, C.; Renard, D.; Robert, P.; Lehr, C. M.; Lamprecht, A.; Hardy, J. Self-assembly of β-lactoglobulin and acacia gum in aqueous solvent: structure and phase-ordering kinetics. *Langmuir* **2002**, *18*, 10323–10333.
3. McNaught, A. D.; Wilkinson, A. *Compendio de Terminologiá Quımíca*; Sintesis: Madrid, Spain, 2003; p117.
4. Weinbreck, F.; de Vries, R.; Schrooyen, P.; de Kruif, C. G. Complex coacervation of whey proteins and gum arabic. *Biomacromolecules* **2003**, *4*, 293–303.
5. Kaibara, K.; Okazaki, T.; Bohidar, H. B.; Dubin, P. L. pH-induced coacervation in complexes of bovine serum albumin and cationic polyelectrolytes. *Biomacromolecules* **2000**, *1*, 100–107.
6. Veis, A.; Aranyi, C. Phase separation in polyelectrolyte systems. I. Complex coacervates of gelatin. *J. Phys. Chem.* **1960**, *64*, 1203–1210.
7. Michaels, A. S.; Miekka, R. G. Polycation-polyanion complexes: preparation and properties of poly(vinyl benzyl trimethyl ammonium) and poly(styrene sulfonate). *J. Phys. Chem.* **1961**, *65*, 1765–1773.
8. Berger, J.; Reist, M.; Mayer, J. M.; Felt, O.; Gurn, R. Structure and interactions in covalently and ionically crosslinked chitosan hydrogels for biomedical applications. *Eur. J. Pharm. Biopharm.* **2004**, *57*, 35–52.
9. Kizilay, E.; Basak-Kayitmazer, A.; Dubin, P. L. Complexation and coacervation of polyelectrolytes with oppositely charged colloids. *Adv. Colloid Interface Sci.* **2011**, *167*, 24–37.
10. Kizilay, E.; Maccarrone, S.; Foun, E.; Dinsmore, A. D.; Dubin, P. L. Clustering in polyelectrolyte-micelle complex coacervation. *J. Phys. Chem. B* **2011**, *115*, 7256–7263.
11. Chollakup, R.; Smitthipong, W.; Eisenbach, C. D.; Tirrell, M. Phase behavior and coacervation of aqueous poly(acrylic acid)- poly(allylamine) solutions. *Macromolecules* **2010**, *43*, 2518–2528.

 doi:10.20944/preprints202407.2533.v1

12. Kayitmazer, A. B.; Strand, S. P.; Tribet, C.; Jaeger, W.; Dubin, P. L. Effect of polyelectrolyte structure on protein-polyelectrolyte coacervates: coacervates of bovine serum albumin with poly-(diallyldimethylammonium chloride) vs. chitosan. *Biomacromolecules* **2007**, *8*, 3568−3577.
13. Bungenberg de Jong, H. G. *In Colloid Science*; Kruyt, H. R., Ed.; Elsevier Publishing: Amsterdam, The Netherlands, 1949; Vol. II, Chapter X, pp 339−432.
14. Luzzi, L. A.; Gerraughty, R. J. Effects of selected variables on the extractability of oils from coacervate capsules. *J. Pharm. Sci.* **1964**, *53*, 429−431.
15. Wang, Q.; Mynar, J. L.; Yoshida, M.; Lee, E.; Lee, M.; Okuro, K.; Kinbara, K.; Aida, T. High-water-content mouldable hydrogels by mixing clay and a dendritic molecular binder. *Nature* **2010**, *463*, 339−343.
16. Tiitu, M.; Hiekkataipale, P.; Hartikainen, J.; Makela, T.; Ikkala, O. Viscoelastic and electrical transitions in gelation of electrically conducting polyaniline. *Macromolecules* **2002**, *35*, 5212−5217.
17. te Nijenhuis, K. Thermoreversible networks: viscoelastic properties and structure of gels. *Adv. Polym. Sci.* **1997**, *130*, 1−267.
18. Burchard, W.; Ross-Murphy, S. B. *Physical Networks: Polymers and Gels;* Elsevier Applied Science: London, UK, 1990.
19. Flory, P. J. Molecular size distribution in three dimensional polymers. I. Gelation. *J. Am. Chem. Soc.* **1941**, *63*, 3083−3090.
20. Stockmayer, W. H. Theory of molecular size distribution and gel formation in branched-chain polymers. *J. Chem. Phys.* **1943**, *11*, 45−55.
21. In *Chemical and Physical Networks: Formation and Control of Properties*; te Nijenhuis, K., Mijs, W. S., Eds.; Wiley: Chichester, UK, 1998; Vol. 1.
22. Lee, S. B.; Lee, Y. M.; Song, K. W.; Park, M. H. Preparation and properties of polyelectrolyte complex sponges composed of hyaluronic acid and chitosan and their biological behaviors. *J. Appl. Polym. Sci.* **2003**, *90*, 925−932.
23. Sankalia, M. G.; Mashru, R. C.; Sankalia, J. M.; Sutariya, V. B. Reversed chitosan-alginate polyelectrolyte complex for stability improvement of α-amylase: optimization and physicochemical characterization. *Eur. J. Pharm. Biopharm.* **2007**, *65*, 215−232.
24. Werle, M.; Takeuchi, H.; Bernkop-Schnurch, A. Modified chitosans for oral drug delivery. *J. Pharm. Sci.* **2009**, *98*, 1643−1656.
25. Sionkowska, A. Current research on the blends of natural and synthetic polymers as new biomaterials: review. *Prog. Polym. Sci.* **2011**, *36*, 1254−1276.
26. Naidu, V. G. M.; Madhusudhana, K.; Sashidhar, R. B.; Ramakrishna, S.; Khar, R. K.; Ahmed, F. J.; Diwan, P. V. Polyelectrolyte complexes of gum kondagogu and chitosan, as diclofenac carriers. *Carbohydr. Polym.* **2009**, *76*, 464−471.
27. Nehdi, I. Characteristics, chemical composition and utilisation of Albizia julibrissin seed oil. *Ind. Crops Prod.* **2011**, *33*, 30–34.
28. Rico Arce, M. L.; Gale, S. L.; Maxted, N. A taxonomic study of Albizia (Leguminosae: Mimosoideae: Ingeae) in Mexico and Central America. *An. Jard. Bot. Madr.* **2008**, 65, 255–305.
29. Aparajita, S.; Rout, G. R. Molecular analysis of Albizia species using AFLP markers for conservation strategies. *J. Genet.* **2010**, *89*, 95–99.
30. Pachuau, L.; Mazumder, B. Albizia procera gum as an excipient for oral controlled release matrix tablet. *Carbohydr. Polym.* **2012**, *90*, 289–295.
31. Nussinovitch, A. Plant Gum Exudates of the World: Sources, Distribution, Properties and Applications, CRC Press, Florida, 2010.
32. Mhinzi, G. S. Properties of gum exudates from selected Albizia species from Tanzania. *Food Chem.* **2002**, *77*, 301–304.
33. Odeku, O. A. Assessment of Albizia zygia gum as a binding agent in tablet formulations. *Acta Pharm.* **2005**, *55*, 263–276.
34. Femi-Oyewo, M. N.; Adedokun, M. O.; Olusoga, T. O. Evaluation of the suspending properties of Albizia zygia gum on sulphadimidine suspension. *Trop. J. Pharm. Res.* **2004**, *3*, 279–284.
35. Pachuau, L.; Lalhlenmawia, H.; Mazumder, B. Characteristics and composition of Albizia procera (Roxb.) Benth gum. *Ind. Crops. Prod.* **2012**, 40, 90–95.
36. De Paula, R. C. M.; Santana, S. A.; Rodrigues, J. F. Composition and rheological properties of Albizia lebbeck gum exudates. *Carbohydr. Polym.* **2001**, *44*, 133–139.
37. Mhinzi, G. S. Properties of gum exudates from selected Albizia species from Tanzania. *Food Chem.* **2002**, *77*, 301–304.
38. De Pinto, G. L.; Martinez, M.; Beltran, O.; Rincon, F.; Clamens, C.; Igartuburu, J. M.; Guerrero, R.; Vera, A. Characterization of polysaccharides isolated from gums of two Venezuelan specimens of Albizia niopoides var. colombiana. *Ciencia* **2002,** *19*, 382–387.
39. Okamoto, Y.; Nose, M.; Miyatake, K.; Sekine, J.; Oura, R.; Shigemasa, Y. Physical changes of chitin and chitosan in canine gastrointestinal tract. *Carbohydr. Polym.* **2001**, *44*, 211−215.

 doi:10.20944/preprints202407.2533.v1

40. Weecharangsan, W.; Opanasopit, P.; Ngawhirunpat, T.; Apirakaramwong, A.; Rojanarata, T.; Ruktanonchai, U.; Lee, R. J. Evaluation of chitosan salts as non-viral gene vectors in CHO-K1 cells. *Int. J. Pharm.* **2008**, *348*, 161−168.
41. Recillas, M.; Silva, L. L.; Peniche, C.; Goycoolea, F. M.; Rinaudo, M.; Argüelles-Monal, W. M. Thermoresponsive behavior of chitosan-g-N-isopropylacrylamide copolymer solutions. *Biomacromolecules* **2009**, *10*, 1633−1641.
42. Pereira, J. L. G. C.; Pais, A. A. C. C.; Redinha, J. S. Maximum likelihood estimation with nonlinear regression in polarographic and potentiometric studies. *Anal. Chim. Acta* **2001**, *433*, 135−143.
43. Ikeda, S.; Kumagai, H.; Sakiyama, T.; Chu, C.; Nakamura, K. Method for analyzing pH-sensitive swelling of amphoteric hydrogels- application to a polyelectrolyte complex gel prepared from xanthan and chitosan. *Biosci., Biotechnol. Biochem.* **1995**, *59*, 1422−1427.
44. Mekhloufi, G.; Sanchez, C.; Renard, D.; Guillemin, S.; Hardy, J. pH-induced structural transitions during complexation and coacerva- tion of β-lactoglobulin and acacia gum. *Langmuir* **2005**, *21*, 386−394.
45. Weinbreck, F.; Nieuwenhuijse, H.; Robijn, G. W.; de Kruif, C. G. Complexation of whey proteins with carrageenan. *J. Agric. Food Chem.* **2004**, *52*, 3550−3555.
46. Tolstoguzov, V. B. Some thermodynamic considerations in food formulation. *Food Hydrocoll.* **2003**, *17*, 1−23.
47. Claesson, P. M.; Ninhami, B. W. pH-dependent interactions between adsorbed chitosan layers. *Langmuir* **1992**, *8*, 1406−1412.
48. Basu, S.; Dasgupta, P. C.; Sircar, A. K. Studies in polyelectrolytes. II. Gum arabate. *J. Colloid Sci.* **1951**, *6*, 539−549.
49. Daniel, C.; Dammer, C.; Guenet, J. M. On the definition of thermoreversible gels: the case of syndiotactic polystyrene. *Polymer* **1994**, *35*, 4243−4246.
50. Molecular Gels: *Materials with Self-Assembled Fibrillar Networks*; Weiss, R. G., Terech, P., Eds.; Springer: Dordrecht, The Netherlands, 2006.
51. Garai, A.; Nandi, A. K. Rheology of polyaniline-dinonylnaphthalene disulfonic acid (DNNDSA) montmorillonite clay nano- composites in the sol state: shear thinning versus pseudo-solid behavior. *J. Nanosci. Nanotechnol.* **2008**, *8*, 1842−1851.
52. Laneuville, S. I.; Turgeon, S. L.; Sanchez, C.; Paquin, P. Gelation of native β-lactoglobulin induced by electrostatic attractive interaction with xanthan gum. *Langmuir* **2006**, *22*, 7351−7357.
53. Bohidar, H.; Dubin, P. L.; Majhi, P. R.; Tribet, C.; Jaeger, W. Effects of protein−polyelectrolyte affinity and polyelectrolyte molec- ular weight on dynamic properties of bovine serum albumin-poly(diallylmethylammonium chloride) coacervates. *Biomacromolecules* **2005**, *6*, 1573−1585.
54. Wang, X.; Lee, J.; Wang, Y.-W.; Huang, Q. Composition and rheological properties of β-lactoglobulin/pectin coacervates: effects of salt concentration and initial protein/polysaccharide ratio. *Biomacromolecules* **2007**, *8*, 992−997.
55. Marudova, M.; McDougall, A. J.; Ring, S. G. Physicochemical studies of pectin/poly-L-lysine gelation. *Carbohydr. Res.* **2004**, *339*, 209−216.